Incorporating replacement free energy of binding-site waters in molecular docking

ARTICLE *in* PROTEINS STRUCTURE FUNCTION AND BIOINFORMATICS · SEPTEMBER 2014

Impact Factor: 2.63 · DOI: 10.1002/prot.24530 · Source: PubMed

4 AUTHORS:

Sun Hanzi
National Institute of Biological Sciences, China
5 PUBLICATIONS **19** CITATIONS
SEE PROFILE

Lifeng Zhao
National Institute of Biological Sciences, China
12 PUBLICATIONS **87** CITATIONS
SEE PROFILE

Shiming Peng
National Institute of Biological Sciences, China
3 PUBLICATIONS **31** CITATIONS
SEE PROFILE

Niu Huang
National Institute of Biological Sciences, China
52 PUBLICATIONS **2,029** CITATIONS
SEE PROFILE

PROTEINS
STRUCTURE ■ FUNCTION ■ BIOINFORMATICS

Incorporating replacement free energy of binding-site waters in molecular docking

Hanzi Sun,[1,2] Lifeng Zhao,[2] Shiming Peng,[2] and Niu Huang[1,2]*

[1] College of Life Sciences, Beijing Normal University, Beijing 100875, China

[2] National Institute of Biological Sciences, Beijing, Zhongguancun Life Science Park, Beijing 102206, China

ABSTRACT

Binding-site water molecules play a crucial role in protein-ligand recognition, either being displaced upon ligand binding or forming water bridges to stabilize the complex. However, rigorously treating explicit binding-site waters is challenging in molecular docking, which requires to fully sample ensembles of waters and to consider the free energy cost of replacing waters. Here, we describe a method to incorporate structural and energetic properties of binding-site waters into molecular docking. We first developed a solvent property analysis (SPA) program to compute the replacement free energies of binding-site water molecules by post-processing molecular dynamics trajectories obtained from ligand-free protein structure simulation in explicit water. Next, we implemented a distance-dependent scoring term into DOCK scoring function to take account of the water replacement free energy cost upon ligand binding. We assessed this approach in protein targets containing important binding-site waters, and we demonstrated that our approach is reliable in reproducing the crystal binding geometries of protein-ligand-water complexes, as well as moderately improving the ligand docking enrichment performance. In addition, SPA program (free available to academic users upon request) may be applied in identifying hot-spot binding-site residues and structure-based lead optimization.

Proteins 2014; 00:000–000.

Key words: binding-site water; molecular dynamics; molecular docking; receptor desolvation energy; binding pose; docking enrichment.

INTRODUCTION

The binding-site water molecules play crucial roles in protein-ligand recognition, either being displaced upon ligand binding or forming water bridges to stabilize the complex.[1–3] Tightly bound waters are often entropically unfavorable due to the restraints imposed by protein binding-site residues; thus, the displacement of such waters into bulky solvents upon ligand binding may result in a favorable entropy gain.[4] However, the enthalpic change may be unfavorable due to the lost of favorable interactions with the protein.[5,6] This leads to the complicated dynamic and thermodynamic behaviors of different binding-site waters.[7] The phenomenon becomes even more complicated in consideration of the bound ligands,[8] therefore, accurately computing the contribution of binding-site water molecules in molecular docking remains challenging.

To include binding-site waters in docking calculation, one promising approach was developed to automatically switch "on" (retain) or "off" (displace) individual water molecule during docking, thus a docked ligand can retain favorable water molecules and displace unfavorable water molecules.[9] It is evident that including binding-site waters in molecular docking improves the binding pose prediction and docking enrichment performance.[10–12] However, the contribution of the majority of binding-site waters are generally neglected by only treating the waters identified to mediate protein-ligand interactions in crystal complex structures. Moreover, it is not clear which waters should be treated as displaceable and which should be treated as fixed in docking, due to the lack of consideration of the water replacement free energy. Nevertheless, efficient yet accurate approaches to incorporate the structural and energetic properties of

Additional Supporting Information may be found in the online version of this article.

Grant sponsor: Chinese Ministry of Science and Technology "973"; Grant number: 2011CB812402; Grant sponsor: National Science Foundation of China; Grant number: 21003011.

*Correspondence to: Niu Huang, National Institute of Biological Sciences, Beijing, No. 7 Science Park Road, Zhongguancun Life Science Park, Beijing 102206, China. E-mail: huangniu@nibs.ac.cn

Received 8 October 2013; Revised 17 January 2014; Accepted 28 January 2014
Published online 7 February 2014 in Wiley Online Library (wileyonlinelibrary.com). DOI: 10.1002/prot.24530

binding-site waters are highly desirable in molecular docking.

In high-throughput docking, a scoring function has to be simple to compute to dock a large chemical library. To be compatible with commonly applied docking algorithms (e.g., rigid receptor and force-field based scoring grids), a reasonable approximation is to neglect the structural perturbation of binding-site residues introduced by bound ligands. Thus, the distributions and energies of individual binding-site waters in an apo-like (ligand unbound state) can be computed prior to docking calculation. A number of physics-based methods have been developed to estimate replacement free energy of binding-site water, including double-decoupling method,[13–16] Inhomogeneous Fluid Solvent Theory,[17,18] 3D-RISM,[19] WaterMap,[20] Just-Add-Water-Molecules,[21] and WaterDock.[22] These methods apply molecular dynamics (MD) or grid-based algorithm to sample the distribution of water molecules inside the protein binding site. The obtained water distribution can be further processed to identify crucial water molecules and to calculate associated energetic properties. Among these approaches, the double-decoupling method is based on free energy perturbation theory,[23] which samples the alchemical pathway between endpoint states (bound state and unbound state) of a specific water in a protein binding site.[16] The computed water replacement free energy using double-decoupling method is generally considered to be the gold standard in the field. More recently, approximate yet efficient methods were developed to sample the endpoint states only. For example, WaterMap software from Schrödinger Inc. simulates the water distribution in a semi-rigid protein binding pocket and then identifies and assigns chemical potentials to each high occupancy water site. This method has been successfully applied in ligand binding affinity prediction and lead compound optimization.[24–29] Knowledge-based methods have also been developed to employ crystallography information to predict the position and energetics of the binding-site waters, including AcquaAlta,[30] DM_hydra,[31] Fold-X,[32] and wPMF.[33] This type of methods is generally efficient and adequate in predicting water location.

Here, we aim to improve the docking performance by treating binding-site water replacement. We wanted to include the predicted binding-site waters in docking, and explicitly treat the water replacement energy in docking scoring function. We first developed the solvent properties analysis (SPA) program to compute the structural and energetic properties of binding-site waters in analog to WaterMap.[20] We investigated the performances of the SPA method in reproducing the structural properties of crystal waters in 124 crystal complex structures,[34] and reproducing the energetic properties of water molecules calculated using double decoupling approach.[15] Next, we implemented a distance-dependent scoring term into DOCK energy function to account for the water replacement free energy cost upon ligand binding. We assessed the new docking scoring function in protein targets containing important binding-site waters, and we demonstrated that our approach can effectively improve the successful rate of reproducing the native binding pose of crystal ligands, as well as moderately improving the ligand docking enrichment performance. Here, we also present anecdotal but encouraging results assessing the ability of more rigorous refinement and rescoring method with the presence of predicted binding-site waters to improve the ligand docking pose prediction. SPA program is free available to academic users upon request, and all our calculation results are open access to scientific community at http://www.huanglab.org.cn/SPA.

MATERIALS AND METHODS

MD simulation protocol

All MD simulations were performed with the program Gromacs (version 4.5.3)[35] using the AMBER99SB force field[36] for protein and TIP3P water model.[37] Protein residues 25 Å away from the ligand were truncated to reduce the size of the simulation system. All crystal waters were removed. The ligand and cofactor, if present, were modeled using the generalized AMBER force field.[38] All calculations applied an atom-based truncation scheme, updated heuristically with a list cutoff of 14 Å, a nonbond cutoff of 12 Å, and the Lennard-Jones smoothing function initiated at 10 Å. Long-range electrostatic interactions were computed using Particle Mesh Ewald method.[39] To equilibrate solvent molecules around the solute, the system was minimized 500 steps using a steepest descent algorithm followed by 200 ps of NVT MD simulation and a subsequent 200 ps of NPT simulation. The 12 ns of NVT MD production simulation was performed at 300 K via the v-rescale temperature coupling scheme. The LINCS algorithm[40] was applied to constrain all bonds involving hydrogen atoms with a time step of 2 fs. All heavy atoms of the protein and ligand were harmonically restrained during the equilibration and production simulation with a force constant of 1000 kJ/mol nm^2.

Water clustering algorithm

Briefly, a spherical volume with a radius of 1 Å is used to cluster all the water molecules in the density profile produced in the MD simulation. Subsequently, a matrix containing the oxygen-oxygen distances of water molecules is derived from the density profile. The spherical volume with the highest water density is chosen as the first hydration site to initiate the iteration process, followed by the removal of all the first hydration site water molecules from the distance matrix and the detection of the second hydration site, the iteration continues until reaching an adequate number of hydration sites (or a user pre-defined number) for further analysis. Finally,

each hydration site is represented by the averaged coordinate of the oxygen atoms of waters within this cluster. The occupancy of the clustered water is computed as the total number of waters identified in this cluster (N_w) divided by the total number of snapshots (N_f) in MD trajectory. Similarly, the hydrogen atoms of each water molecule are also clustered, and the top two clusters of the hydrogen atoms of each hydration site are used to present the positions and orientations of the hydrogen atoms and to generate the hydrogen bond properties of water molecules.

Replacement free energy calculation of binding-site water

Water replacement free energy (ΔG_{SPA}) is defined as the free energy penalty of removing a specific water molecule from the binding site to the bulk water [Eq. (1)]. This can be decomposed into two energy components (ΔG_{cavity} and ΔG_{bulk}), representing the energy penalties to remove the water molecule from protein cavity and bulk environment into vacuum, individually. We first calculated the free energy cost of decoupling a TIP3P water molecule from bulk solvent (ΔG_{bulk}) using the thermodynamic integration method. The standard deviation is calculated as the integration of energy deviation during each perturbation steps along the alchemical transformation pathway. The computed free energies of eliminating the electrostatic interactions and vdW interactions are 8.2 ± 0.2 and −2.1 ± 0.1 kcal/mol, yielding a total free energy of 6.1 ± 0.2 kcal/mol.

The free energy to decouple binding-site water (ΔG_{cavity}) can be decomposed into the direct energy cost to eliminate the water molecule ($\Delta G_{decoupling}$) and the indirect energy expense to reorganize the binding-site water network after removing the water molecule ($\Delta G_{reorganization}$). The enthalpy and entropy components of decoupling energy $\Delta G_{decoupling}$ are calculated separately, where the enthalpy part is estimated by the interaction energy between the target water and the rest of the entire system, including the vdW interactions ($vdW_{w\text{-}s}$ and $vdW_{w\text{-}w}$) and electrostatic interactions ($ele_{w\text{-}s}$ and $ele_{w\text{-}w}$), individually; the entropy change during decoupling of the water ($T\Delta S$) is calculated using a simplified inhomogeneous fluid solvation theory [Eq. (2)].[18,20] In this equation, the partial excess entropy is calculated by numerically integrating an expansion of the translational entropy [first term in Eq. (2)] and orientational entropy [second term in Eq. (2)]. For each hydration site, the water's local density is derived from the translational correlation function $g_{sw}(r)$ with respect to the spherical coordinates (r, θ, and φ) using bulk water density as the reference state. Thus, the translational entropy is calculated using the precomputed water density map, where each spherical coordinate is divided into 5 bins, resulting to total of 125 sub fractions. Similarly, the hydrogen atom density map is used to calculate water orientational entropy, where $g_{sw}(\omega)$ is the orientational correlation function derived from the Euler angles of the water in each hydration site. Three orientational coordinates (θ, φ, and ψ) are divided into 4, 4, and 2 bins respectively, which leads to 16 fractions for each hydration site with consideration of the symmetrical characteristics of water molecule.

The reorganization energy ($\Delta G_{reorganization}$) is challenging to calculate directly, therefore, we developed a scaling scheme to estimate this energy term by scaling the vdW interaction energy terms and electrostatic interaction terms accordingly [Eq. (1)]. We optimized the scaling factors by benchmarking against the data set published by Barillari et al.[15] where the authors computed the water replacement free energy for 54 binding-site waters using double decoupling method. We further assessed our optimized scaling factor using the experimentally determined water transfer energy from bulk to vacuum (6.3 kcal/mol).[41] After parameter optimization, the scaling factors a, b, and c were set to be 0.2, 0.3, and 0.6, individually, which led to the final SPA energy function [Eq. (3)]. For a bulk water, the calculated ΔG_{SPA} is −0.06 kcal/mol (electrostatic and vdW interaction energies with surrounding environment are −20.4 and 2.5 kcal/mol, individually), which indicates the small systematic error of our SPA energy function.

$$\begin{aligned}\Delta G_{SPA} &= \Delta G_{cavity} + \Delta G_{bulk} \\ &= \Delta G_{decoupling} + \Delta G_{reorganization} + \Delta G_{bulk} \\ &= [vdW_{W-S} + ele_{W-S} + vdW_{W-W} + ele_{W-W} \\ &\quad + T\Delta S] - [a * (vdW_{W-S} + vdW_{W-W}) \\ &\quad + b * ele_{W-S} + c * ele_{W-W}] + \Delta G_{bulk}\end{aligned} \tag{1}$$

$$\begin{aligned}\Delta S = S^e &\approx -k_b \rho_w \int g_{sw}(r)\ln(g_{sw}(r))\,dr \\ &\quad - \frac{k_b N_w^V}{\Omega}\int g_{sw}(\omega)\ln(g_{sw}(\omega))\,d\omega\end{aligned} \tag{2}$$

$$\begin{aligned}\Delta G_{SPA} &= 0.8 * (vdW_{W-W} + vdW_{W-S}) + 0.7 * ele_{W-S} \\ &\quad + 0.4 * ele_{W-W} + T\Delta S + 6.1\end{aligned} \tag{3}$$

Water structural and energetic properties calculation

We assembled two testing data sets to validate the performance of SPA on reproducing structural properties and calculating energetic properties of binding-site waters, respectively. To assess the propensities on predicting the geometry and mobility of binding-site waters, a total of 124 crystal complex structures were chosen from the CSAR-NRC HiQ data set (Supporting Information Table S1), where the criteria were defined as crystal resolution better than 2.5 Å, at least 5 crystal waters and no

ions presenting in the binding site (5 Å around heavy atoms of the crystal ligand). The replacement free energies of 54 water molecules in 35 crystal structures of 6 different proteins were calculated and compared with the energy values reported in the literature using double decoupling calculation method.[15] All data sets and related calculation results presented in this study are open access at http://www.huanglab.org.cn/SPA.

Water replacement in docking

The structural and energetic properties of first-shell waters were computed using SPA method for each protein target in unbound state, where qualified water forms at least one hydrogen bond with binding-site residues or the calculated occupancy of water molecule is >30%. Docking was performed using an in-house modified version of program DOCK 3.5.54[42–44] to generate docking poses and to score library compounds with the presence of predicted stable first-shell binding-site waters. DOCK 3.5.54 is a flexible-ligand docking method designed to efficiently sample the ligand conformational space, where ensembles of pre-calculated conformers are used to significantly speed up docking calculations.[42] On average, sampling millions of poses for a single ligand takes less than one second. Note that the docking spheres were generated without the presence of any predicted binding-site waters, and thus ligand sampling is identical to docking against a naked binding pocket. A water molecule is replaced if the distance between the oxygen atom of the water molecule and any heavy atom of docked ligand is less than the predefined expulsion radius of this heavy atom. The expulsion radius of different ligand atom types were determined empirically by surveying 66,559 PDB crystal structures (Supporting Information Fig. S1). Ligand conformations are scored after the sampling and the rigid minimization based on the docking total energy ($E_{tot} = E_{ele} + E_{vdw} - \Delta G_{lig\text{-}solv} - \Delta G_{rec\text{-}solv}$), which is the sum of electrostatic (E_{ele}) and van der Waals (E_{vdw}) interaction energies between protein and ligand corrected by the ligand partial desolvation energy ($\Delta G_{lig\text{-}solv}$) and the receptor partial desolvation energy ($\Delta G_{rec\text{-}solv}$). The ligand partial desolvation energy is calculated as the sum of the partial atomic desolvation energies as previously described, where the atomic desolvation energy was precalculated for each ligand using AMSOL program,[43] and the partial atomic desolvation energy was based on the fraction of surface area buried by the receptor for any given ligand atom.[44] And the receptor partial desolvation energy term is calculated as the sum of replacement free energies of individual water multiplied by its occupancy [Eq. (4)]. Note that the free energy of ligand desolvation may be estimated in the same manner as our receptor partial desolvation calculation, as recently reported.[45] Unfortunately, explicit treatment of ligand solvation shell will be extremely difficult to be implemented in high throughput docking method treating millions of different ligands. On contrast, it is feasible to calculate the water distribution and energy property of an invariant receptor binding-site, and incorporated as an approximated solution of receptor desolvation in docking. A single docking pose with the best total energy score is saved for each docked molecule. Nevertheless, this energy term can be easily incorporated into other docking scoring functions, or can be used in a postdock rescoring stage.

$$\Delta G_{rec-solv} = \sum_{i=1}^{N_E} \Delta G_{SPA}(i) * Occupancy(i) \qquad (4)$$

Assessment of the new scoring function

Docking performance was assessed by reproducing the binding poses of the crystal ligands, and by enriching the true ligands among top scoring docked molecules from a database of decoys. For binding pose assessment, eight drug targets were selected based on the availability of binding-site waters, total of 191 crystal complex structures (Supporting Information Table S2). To evaluate the docking enrichment, we selected 27 targets from the Directory of Useful Decoys (DUD) data set,[46] and calculated the enrichment factor at 1% (EF_1) and receiver operator characteristic based LogAUC.[47] An automated docking pipeline was applied in all docking calculations as described previously.[46,48]

Protein-water-ligand complex structure refinement

The docked protein-water-ligand complex structure was submitted to a physics-based refinement procedure using the Protein Local Optimization Program (PLOP) with an all-atom molecular-mechanics (MM) force field and a generalized Born surface area (GB/SA) implicit solvent model.[46,49–51] All the protein heavy atoms were kept rigid, and the docked ligand and waters were fully relaxed during minimization.

RESULTS AND DISCUSSION

The automated SPA pipeline

As illustrated in Figure 1, the SPA calculation starts from building a water oxygen density map based on MD simulation trajectory, followed by water oxygen clustering using a bin size of 1 Å. After obtaining the position of each water cluster, the orientation of hydrogen atoms of each water molecule is analyzed for building the local hydrogen bonding network. Finally, the energetic properties of each water cluster are calculated and reported along with its structural information, which is

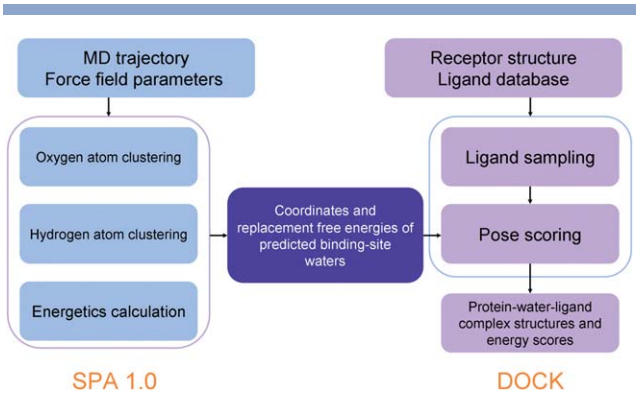

Figure 1

Flowchart of implementation of water replacement free energy calculation in molecular docking. [Color figure can be viewed in the online issue, which is available at wileyonlinelibrary.com.]

automatically ported into the molecular graphics program UCSF Chimera[52] for graphical visualization. For example, eight binding-site waters identified by SPA are correctly located within 1 Å distance cutoff of corresponding crystal waters in adipocyte fatty acid binding protein (αFABP) complex structure [Fig. 2(A)]. 15 of 17 binding-site waters in apo crystal structure were correctly identified within 1 Å distance cutoff using an apo-like structure (i.e., excluding the bound ligand) [Fig. 2(B)], and all 17 waters could be identified if the distance cutoff was relaxed to 1.5 Å.

Structural and dynamic properties of water molecules

The accurate prediction of the location and orientation of important binding-site water molecules is essential for accounting the water's energetic contribution in ligand docking; therefore, we first assessed the SPA performance to reproduce the spatial location and the experimentally determined local mobility of 1228 binding-site waters in 124 crystal complex structures (Table I). The predictive rates (i.e., probability of crystal waters to be reproduced) are satisfactory, ranging from 62.1 to 75.4% depending on the evaluation criteria. Although it is not an "apple-to-apple" comparison due to the different data sets and different cutoff criteria, the accuracy performance of our approach is in the same range as reported in other work. For example, the prediction accuracy of binding-site waters is 76.2% using an empirical function-based method AcquaAlta,[30] and is 81% using an energy scoring function-based algorithm WaterDock,[22] respectively. The true positive rates (i.e., propensity of predicted waters to be crystal waters) are lower than the predictive rates. The difference between our prediction and the crystal structure may be partly

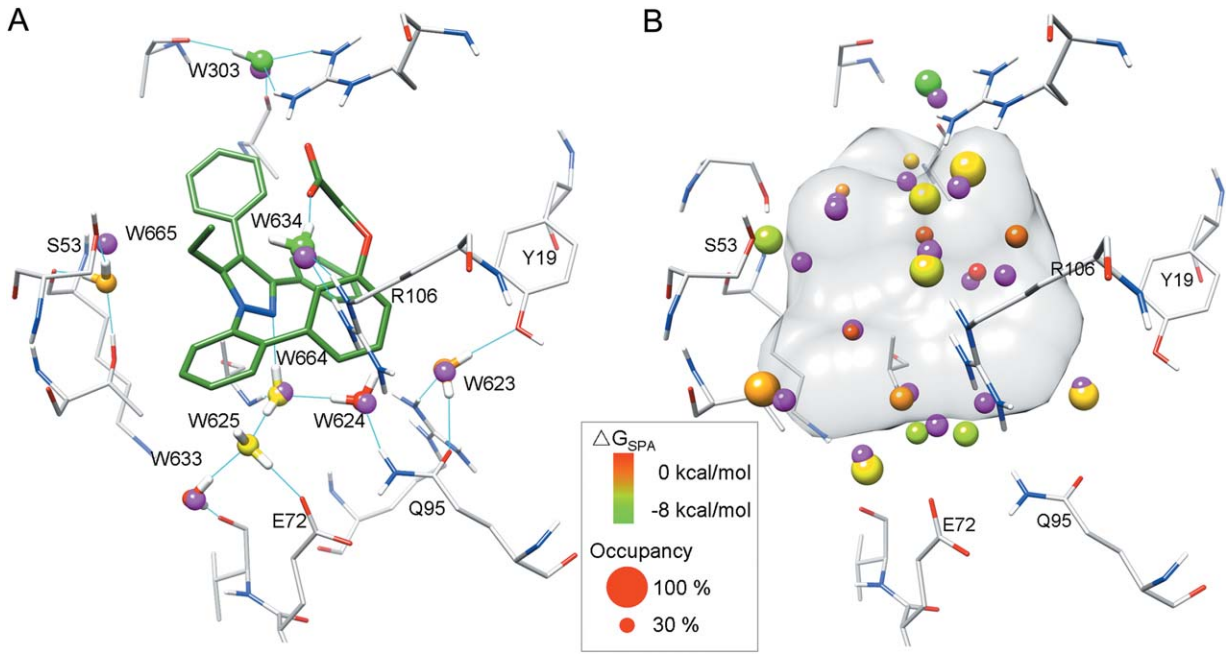

Figure 2

Predicted binding-site waters in (**A**) crystal complex structure of αFABP (PDB ID: 2NNQ) and (**B**) corresponding apo-like structure (excluding the ligand). The crystal ligand is colored in forest green, the crystal waters are colored in magenta, and the protein residues are colored in light gray. Note that the crystal waters from an apo structure (PDBID: 3Q6L) are included in the apo-like system for comparison. The predicted binding-site water is colored based on the calculated replacement free energy ΔG_{SPA}, from unfavorable (red) to highly favorable (green), and its calculated occupancy is represented by its size of the oxygen atom. Molecular images were generated with UCSF Chimera.

Table I
Structural Prediction Accuracy Assessment in Reproducing 1,228 Crystal Waters in 124 Crystal Structures

Distance cutoff (Å)	Occupancy cutoff	Predictive rate	True positive rate
1	30%	62.1	41.8
1.5	30%	75.4	52.8

due to the static crystal structure (PDB coordinate) presenting waters as either present or absent. Calculation results shall always consult with critical examination of electron density, especially the weak electron density regions for any specific target of interest. Although not explicitly investigated at present study, we noted that removing the crystal waters during the system preparation does have a negative impact on the prediction accuracy; ~10% of crystal waters could not be identified using the current standard water addition algorithm (data not shown).

Further structural analysis shows that for crystal water molecules with lower temperature factor (B factor), the predictive rate is higher [Fig. 3(A)]; and in crystal structures with higher crystallographic resolution, the true positive rate is also higher [Fig. 3(B)]. In nine structures with crystallographic resolution better than 1.5 Å, the predictive rate is 83.5% and true positive rate is 79.8%. These results suggest some binding-site waters might not be modeled robustly in the crystal structure due to their lower stability or the limited crystallographic resolution of the structure. Similar observation had been discussed in other published work.[22,31] Nevertheless, the predicted water molecules with higher occupancy also show higher true positive rate [Fig. 3(C)], which is consistent with one of the basic roles in the field of crystallography, the physically more stable water molecules are more likely to be modeled into the crystal structure.[53]

Replacement free energy of binding-site waters

The replacement free energy (ΔG_{SPA}) of each water cluster is calculated using the SPA energy function described in the methodology section [Eq. (3)]. Although SPA approach is a physically less profound method, the calculated water replacement free energy values show good correlation with the energies calculated using more complicated double decoupling method, with a correlation coefficient R^2 of 0.62 and a RMSD of 2.28 kcal/mol. Notably, the average energy difference is small, only 0.38 kcal/mol (Fig. 4).

Evaluation of ligand pose prediction

We expected that our docking scoring function with inclusion of water replacement energy term might improve the docking performance in discriminating native-like poses from wrongly docked poses. The docking pose accuracy was assessed based on the root-mean-square deviation (RMSD) values between the coordinates of the heavy atoms in the ligands in the top 1 scoring pose and the native crystallographic pose, and a cutoff value of 2 Å was chosen to discriminate the docking success from failure. In our testing data set containing 8 different drug targets, total of 191 protein-ligand complex structures, the success rate of predicting near-native binding pose increased from 44.5% of the targets to 55.5%. The detailed results are summarized in Table II.

We carefully checked the poses resulted from our new scoring method in comparison with the original DOCK scoring function (Supporting Information Fig. S2). The improvement is more significant in targets such as human heat shock protein 90 (HSP90) and proviral integration site in Moloney murine leukemia virus (PIM1) kinase (Table II) where the binding-site waters are essential for ligand binding.[54,55] Clearly, the addition of water replacement free energy may remove certain bias

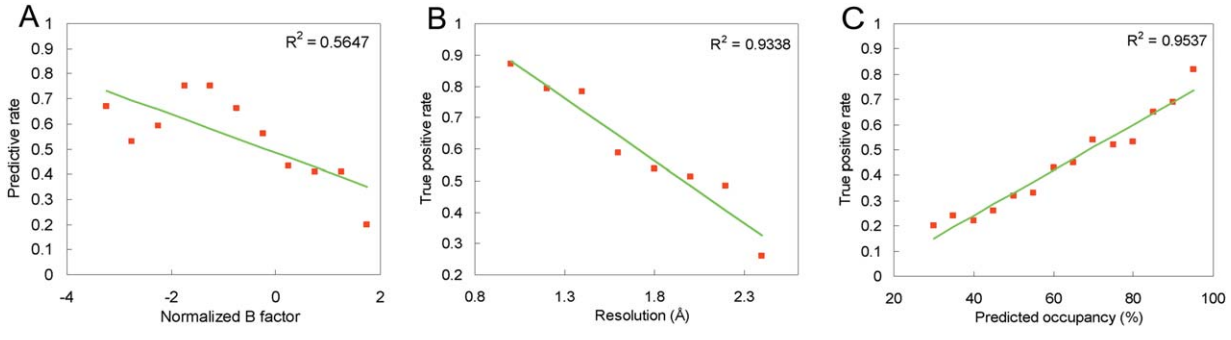

Figure 3
Correlation between (**A**) the normalized experimental B factor of crystal waters and the predictive rate; (**B**) the crystallographic resolution and the true positive rate of predicted waters and (**C**) the predicted water occupancy and the true positive rate. Predictive rate and true positive rate are calculated using distance cutoff equal to 1.5 Å and occupancy cutoff equal to 30%. [Color figure can be viewed in the online issue, which is available at wileyonlinelibrary.com.]

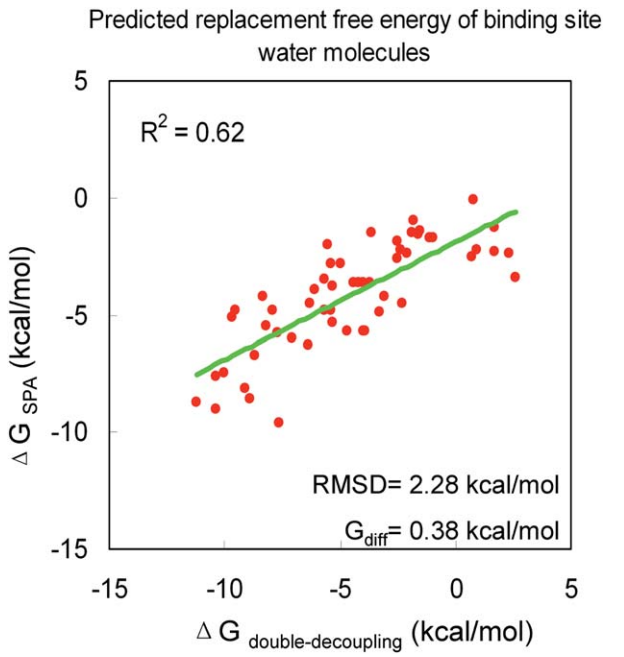

Figure 4

Correlation between water replacement free energy calculated using SPA (ΔG_{SPA}) and double decoupling method ($\Delta G_{double\text{-}decoupling}$). [Color figure can be viewed in the online issue, which is available at wileyonlinelibrary.com.]

toward the wrongly docked poses caused by the simple docking scoring function. For example, without the correction of water replacement, the top one docking pose deviates significantly from the native pose (RMSD = 6.91 Å) in one HSP90 structure (PDBID: 1UY7) as shown in Figure 5(A), where misdocked ligand forms hydrogen bond with residue K58 and contacts favorably with residues L48 and V186, displacing four stable binding-site waters (W1, W2, W3, and W4) [Fig. 5(A)], which are highly conserved in HSP90 crystal complex structures. In striking contrast, with the consideration of the water replacement energy term, the native-like pose is correctly scored as the top one docking pose with an RMSD of 1.01 Å [Fig. 5(B)]. The misdocked pose requires compensating 22.47 kcal/mol to replace the binding-site waters, while the native-like pose only pays energy cost of 6.84 kcal/mol. Similarly, in PIM1 kinase (PDBID: 2XIZ), the top one docking pose is misdocked with an RMSD value of 10.65 Å without accounting the energy penalty of 11.02 kcal/mol [Fig. 5(C)]. The consideration of the water replaceable free energy term dramatically improves the docking pose with an RMSD of 0.61 Å by only paying energy penalty of 5.13 kcal/mol [Fig. 5(D)]. The similar results are also observed in other targets [Supporting Information Fig. S3(A–D)].

It is well known that using RMSD cutoff as the only criterion to evaluate docking pose fidelity is not comprehensive, considering that even subtle difference of the binding pose may lead to the large deviation of the docking energy. By carefully checking all docking poses, we found that the inclusion of water replacement energy term in scoring function improves the native pose reproduction not only judging from RMSD, but also from the microscopic interactions such as critical polar and apolar interactions (Table III). As shown in Figure 6(A), the top one docking pose from original DOCK reproduces the overall binding characteristics of crystal ligand in a HSP90 structure (PDBID: 2WI3) except the misdocked methylthio group. The position of this methylthio group is correctly predicted by including the replacement free energy cost of a deeply buried water molecule (W5, 2.4 kcal/mol) [Figure 6(B)]. Such fine adjustments of docking poses can be also found in other cases (Supporting Information Fig. S3(E,F)].

Ligand enrichment performance in DUD data set

Another key measure of the docking performance is the enrichment of ligands among the top ranking docked molecules. We tested our new scoring method in screens of 27 DUD targets.[46] On average, incorporation of water replacement free energy term improves the enrichment factor EF1 by 0.38 and LogAUC by 0.32 (Fig. 7). The

Table II

Docking Pose Accuracy Assessment of Including the Water Replacement Energy Term in Docking Scoring Function (a RMSD Cutoff Value of 2 Å is Chosen to Discriminate the Docking Success from Failure)

Target	Number of crystal structures	Correctly reproduced by original DOCK scoring function	Correctly reproduced by inclusion of water replacement energy term	Correctly reproduced in both scoring functions
CHK1	29	20	24	5
DPP4	20	13	12	8
GPB	21	5	7	1
HSP90	36	17	26	4
PIM1	21	11	16	6
PPARg	30	8	8	6
PTP1B	18	7	7	5
THROMBIN	16	4	6	3
Over all	191	85	106	38

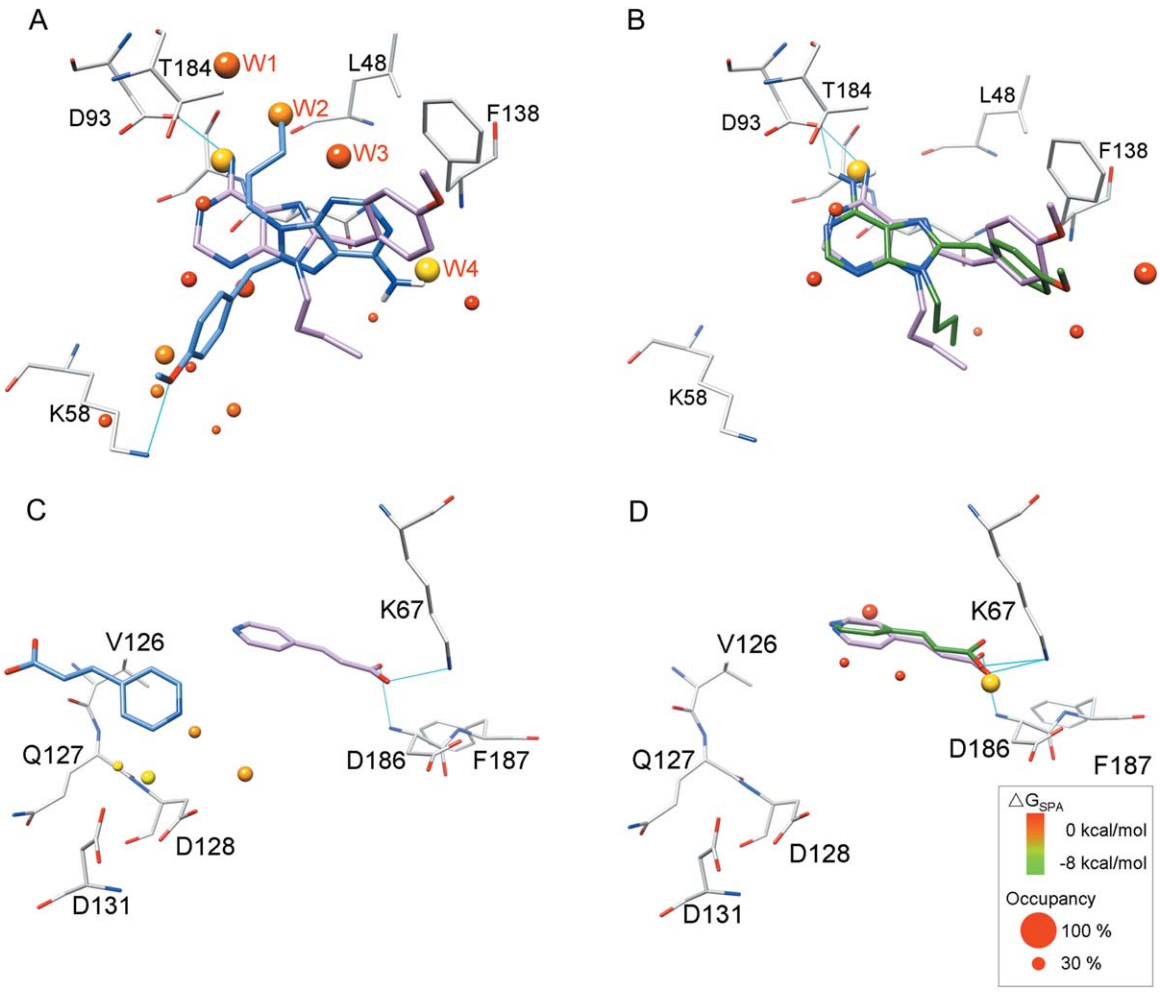

Figure 5

The top one docking pose obtained from original DOCK scoring function (colored in blue) or scoring function corrected by the water replacement energy term (colored in green) in HSP90 (PDBID: 1UY7) and PIM1 (PDBID: 2XIZ). Crystal ligand pose is colored in pink. Only water molecules replaced by the docked ligand are highlighted.

most significance case is HIV reverse transcriptase (HIVRT), where the EF1 is improved by 7.92 and LogAUC is improved by 3.47. It is likely that the improved enrichment performance is resulted from the improved binding pose reproduction. In HIVRT, the native binding poses in 40 structures are correctly reproduced among 64 complex structures with the addition of water replacement free energy term, 21% improvement

Table III

Improved Pose Prediction Accuracy Using Docking Scoring Function with the Water Replacement Energy Correction

				Top one docking pose (without correction)		Top one docking pose (with correction)	
Target	PDBID	RMSD (without correction) (Å)	RMSD (with correction) (Å)	Original DOCK score (kcal/mol)	Water replacement energy term (kcal/mol)	Original DOCK score (kcal/mol)	Water replacement energy (kcal/mol)
CHK1	2XEZ	6.30	1.13	−30.90	12.17	−29.79	5.85
HSP90	1UY7	6.91	1.01	−36.39	22.47	−32.01	6.84
HSP90	1UYC	6.82	0.58	−33.39	20.55	−31.60	7.09
HSP90	2WI3	3.49	0.40	−23.62	12.65	−21.60	10.42
PIM1	2XIZ	10.65	0.63	−0.35	11.02	3.21	5.13
PIM1	3CY2	4.17	0.24	−55.34	14.77	−54.01	12.35
PPARg	3NOA	11.96	1.30	0.07	17.14	5.34	8.88
Thrombin	2CF9	3.25	1.36	−74.02	19.99	−73.82	18.29

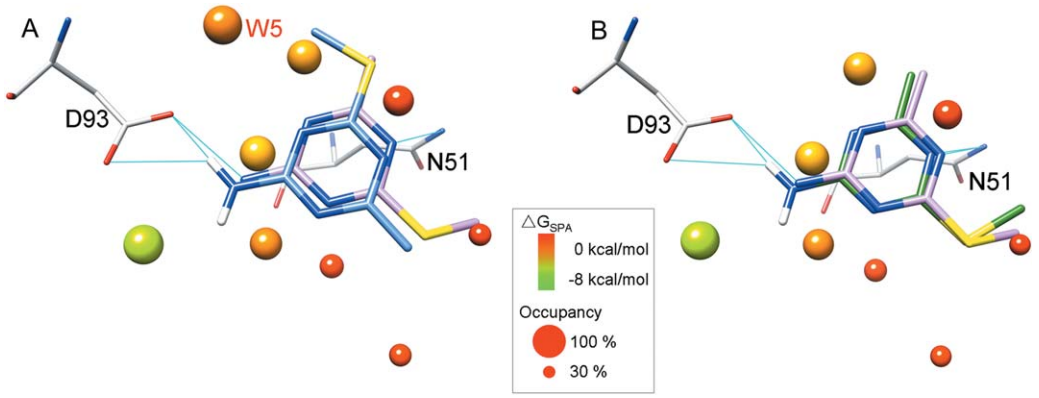

Figure 6

The top one docking pose obtained from original DOCK scoring function (colored in blue) or scoring function corrected by the water replacement energy term (colored in green) in HSP90 (PDBID:2WI3). Crystal ligand pose is colored in pink. Only water molecules replaced by the docked ligand are highlighted.

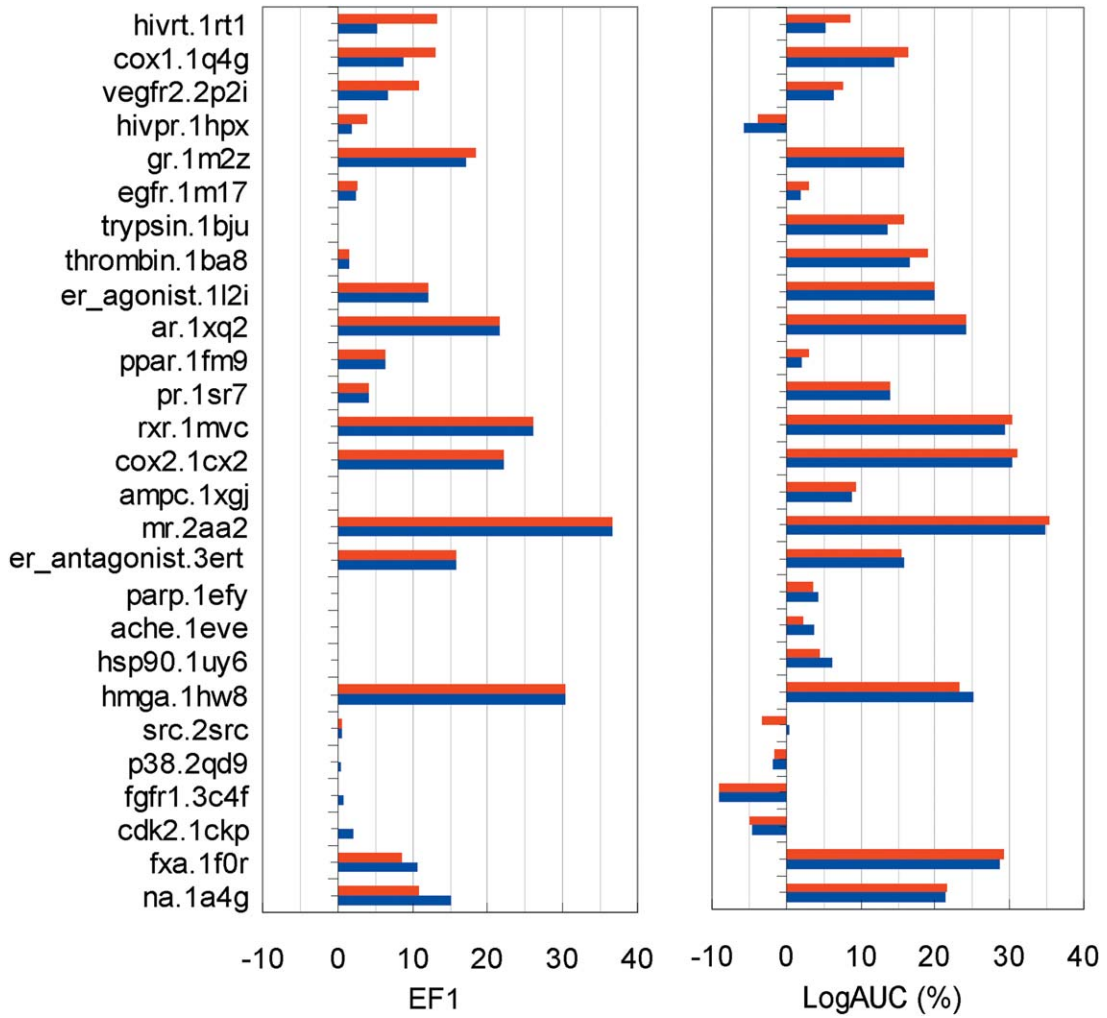

Figure 7

EF1 and LogAUC obtained from docking with (colored in red) or without (colored in blue) the inclusion of the water replacement energy term in 27 DUD targets. [Color figure can be viewed in the online issue, which is available at wileyonlinelibrary.com.]

than using original DOCK scoring function. We also identified cases like HSP90, where the improvement in reproducing the native pose does not necessarily lead to the improvement of enrichment performance. Visually examination of the docking poses of highly scored decoys indicates that most top ranking decoy molecules are artificially docked on the protein surface residues where the replacement of water molecules is not penalized in our current scoring scheme. The bias in this case most likely arises from the overestimated polar interactions between ligand and protein surface residues.

Postdocking refinement

In principle, a hierarchical docking screening strategy shall work better by integrating different computational methods in an increasing order of complexity and more physically realistic manner.[56–58] Here, we also present anecdotal but encouraging results assessing the ability of more rigorous refinement and rescoring method with the presence of predicted binding-site waters to improve the ligand docking pose prediction. For example, bridging waters are critical in mediating the protein-ligand interactions in HSP90 (PDBID: 1UY7). Since the binding-site waters were predicted in ligand unbound state, some of these predicted waters are not precisely located and oriented as in the crystal complex structures. Ligand optimization along with binding-site waters using MM-GB/SA refinement procedure not only further reduces the RMSD of ligand docking pose to 0.7 Å, also precisely reproduces the hydrogen bond network forming between protein, ligand and mediating waters by adjusting the water's position and orientation [Fig. 8(A)]. The relocation of water molecules is even more obvious in checkpoint kinase-1 (CHK1) [Fig. 8(B)], one water molecule (W6) shifts about 1.2 Å to form better interactions with the surrounding environment, and the ligand binding pose is improved from RMSD value of 1.2 to 0.4 Å, correspondingly.

Time cost of adding new energy term

In enrichment calculation, the average time cost to screen 89,611 DUD molecules against one binding site using original DOCK3.5.54 is 24.5 CPU hours, the addition of water replacement free energy term only increases 3.6 CPU hours by calculating the pair-wise distances between each predicted water molecule and the heavy atoms of docked ligands.

CONCLUSION

Rigorously treating explicit binding-site waters is challenging in molecular docking. Therefore, an efficient yet accurate method to computationally predict the structural and energetic properties of binding-site waters is desirable. Here, we developed the SPA program to compute the structural and energetic properties of binding-site waters by post-processing MD trajectories. The water replacement free energy calculated using the SPA method

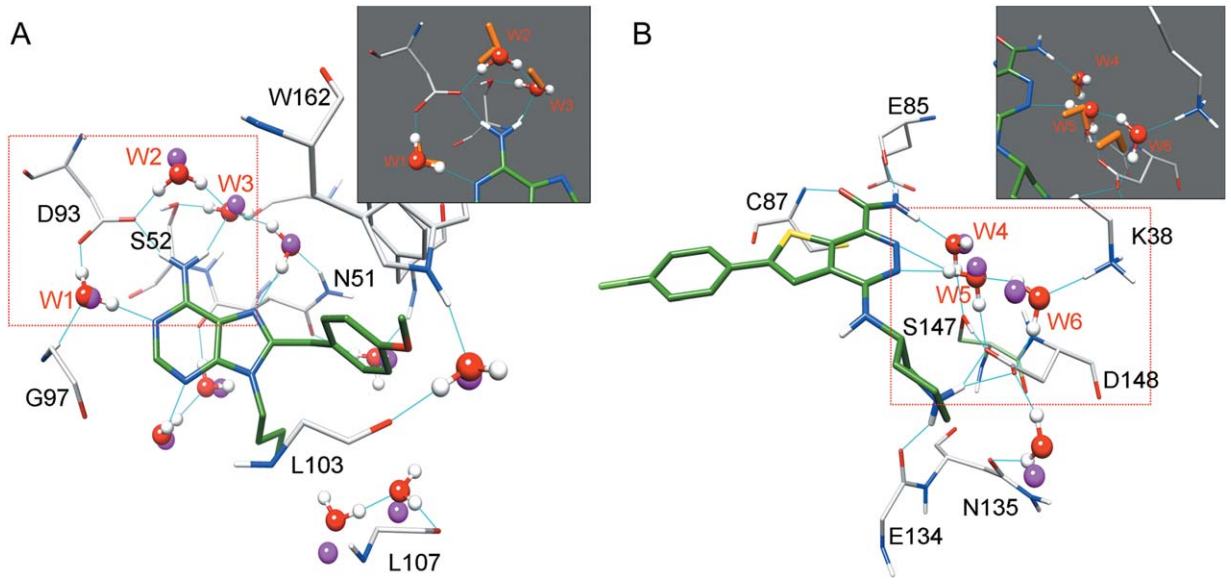

Figure 8

The docked protein-water-ligand structures of (**A**) HSP90 (PDBID: 1UY7) and (**B**) CHK1 (PDBID: 3PA3). Water molecules obtained directly from docking are colored in orange and shown in the top gray panel for comparison. Waters optimized along with the docked ligand are shown in ball and stick model with oxygen atoms colored in red, and hydrogen atoms colored in white. Crystal waters obtained from the crystal complex structure are colored in magenta. Minimized docking poses are colored in green.

is comparable to more rigorous free energy calculation approaches like double decoupling method. Nevertheless, it is a highly efficient approach, only takes <3 h to compute the energetics of all identified waters in one binding site. Note that all reported SPA results presented in the current study are open access to scientific community at http://www.huanglab.org.cn/SPA/. We expect that such water properties analysis approach shall not be limited in studying protein-ligand binding interactions. We have recently applied this method to investigate water behaviors on the surface of DNA, and to facilitate our understanding of the thermodynamic basis of altered stability of selenium-modified DNA.[59]

More importantly, we developed a highly efficient distance-dependent energy term to include the water replacement energy cost in DOCK scoring function. The docking pose accuracy performance is significantly improved in targets including HSP90, PIM1, CHK1, and HIVRT. We also noted that the docked poses are improved not only judging from RMSD values of all heavy atoms, also from the microscopic atomic details such as critical polar and apolar interactions. The consideration of the new energy term modestly improves the performance of docking program in ligand enrichment test. In addition, the generated protein-water-ligand ternary complex structure might be useful in postdock analysis or structure refinement using higher level scoring methodologies.

ACKNOWLEDGMENT

Computational support was provided by the Supercomputing Center of Chinese Academy of Sciences (SCCAS).

REFERENCES

1. Lu Y, Wang R, Yang CY, Wang S. Analysis of ligand-bound water molecules in high-resolution crystal structures of protein-ligand complexes. J Chem Inf Model 2007;47:668–675.
2. Mancera RL. Molecular modeling of hydration in drug design. Curr Opin Drug Discov Devel 2007;10:275–280.
3. Wong SE, Lightstone FC. Accounting for water molecules in drug design. Expert Opin Drug Discov 2011;6:65–74.
4. Lam PY, Jadhav PK, Eyermann CJ, Hodge CN, Ru Y, Bacheler LT, Meek JL, Otto MJ, Rayner MM, Wong YN, Chang CH, Weber PC, Jackson DA, Sharpe TR, Viitanen SE. Rational design of potent, bioavailable, nonpeptide cyclic ureas as HIV protease inhibitors. Science 1994;263:380–384.
5. Clarke C, Woods RJ, Gluska J, Cooper A, Nutley MA, Boons GJ. Involvement of water in carbohydrate-protein binding. J Am Chem Soc 2001;123:12238–12247.
6. Kadirvelraj R, Foley BL, Dyekjaer JD, Woods RJ. Involvement of water in carbohydrate-protein binding: concanavalin A revisited. J Am Chem Soc 2008;130:16933–16942.
7. Knight JD, Hamelberg D, McCammon JA, Kothary R. The role of conserved water molecules in the catalytic domain of protein kinases. Proteins 2009;76:527–535.
8. Singh N, Warshel A. A comprehensive examination of the contributions to the binding entropy of protein-ligand complexes. Proteins 2010;78:1724–1735.
9. Rarey M, Kramer B, Lengauer T. The particle concept: placing discrete water molecules during protein-ligand docking predictions. Proteins 1999;34:17–28.
10. Huang N, Shoichet BK. Exploiting ordered waters in molecular docking. J Med Chem 2008;51:4862–4865.
11. Kumar A, Zhang KY. Investigation on the effect of key water molecules on docking performance in CSARdock exercise. J Chem Inf Model 2013;53:1880–1892.
12. Verdonk ML, Chessari G, Cole JC, Hartshorn MJ, Murray CW, Nissink JW, Taylor RD, Taylor R. Modeling water molecules in protein-ligand docking using GOLD. J Med Chem 2005;48:6504–6515.
13. Zhang L, Hermans J. Hydrophilicity of cavities in proteins. Proteins 1996;24:433–438.
14. Hamelberg D, McCammon JA. Standard free energy of releasing a localized water molecule from the binding pockets of proteins: double-decoupling method. J Am Chem Soc 2004;126:7683–7689.
15. Barillari C, Taylor J, Viner R, Essex JW. Classification of water molecules in protein binding sites. J Am Chem Soc 2007;129:2577–2587.
16. Yu H, Rick SW. Free energies and entropies of water molecules at the inhibitor-protein interface of DNA gyrase. J Am Chem Soc 2009;131:6608–6613.
17. Li Z, Lazaridis T. The effect of water displacement on binding thermodynamics: concanavalin A. J Phys Chem B 2005;109:662–670.
18. Li Z, Lazaridis T. Thermodynamic contributions of the ordered water molecule in HIV-1 protease. J Am Chem Soc 2003;125:6636–6637.
19. Imai T, Hiraoka R, Kovalenko A, Hirata F. Locating missing water molecules in protein cavities by the three-dimensional reference interaction site model theory of molecular solvation. Proteins 2007;66:804–813.
20. Abel R, Young T, Farid R, Berne BJ, Friesner RA. Role of the active-site solvent in the thermodynamics of factor Xa ligand binding. J Am Chem Soc 2008;130:2817–2831.
21. Michel J, Tirado-Rives J, Jorgensen WL. Prediction of the water content in protein binding sites. J Phys Chem B 2009;113:13337–13346.
22. Ross GA, Morris GM, Biggin PC. Rapid and accurate prediction and scoring of water molecules in protein binding sites. PLoS One 2012;7:e32036.
23. Gilson MK, Given JA, Bush BL, McCammon JA. The statistical-thermodynamic basis for computation of binding affinities: a critical review. Biophys J 1997;72:1047–1069.
24. Beuming T, Farid R, Sherman W. High-energy water sites determine peptide binding affinity and specificity of PDZ domains. Protein Sci 2009;18:1609–1619.
25. Pearlstein RA, Hu QY, Zhou J, Yowe D, Levell J, Dale B, Kaushik VK, Daniels D, Hanrahan S, Sherman W, Abel R. New hypotheses about the structure-function of proprotein convertase subtilisin/kexin type 9: analysis of the epidermal growth factor-like repeat A docking site using WaterMap. Proteins 2010;78:2571–2586.
26. Abel R, Salam NK, Shelley J, Farid R, Friesner RA, Sherman W. Contribution of explicit solvent effects to the binding affinity of small-molecule inhibitors in blood coagulation factor serine proteases. ChemMedChem 2011;6:1049–1066.
27. Beuming T, Che Y, Abel R, Kim B, Shanmugasundaram V, Sherman W. Thermodynamic analysis of water molecules at the surface of proteins and applications to binding site prediction and characterization. Proteins 2012;80:871–883.
28. Robinson DD, Sherman W, Farid R. Understanding kinase selectivity through energetic analysis of binding site waters. ChemMedChem 2010;5:618–627.
29. Li J, Du Y, Liu X, Shen QC, Huang AL, Zheng MY, Luo XM, Jiang HL. Binding sensitivity of adefovir to the polymerase from different

genotypes of HBV: molecular modeling, docking and dynamics simulation studies. Acta Pharmacol Sin 2013;34:319–328.
30. Rossato G, Ernst B, Vedani A, Smiesko M. AcquaAlta: a directional approach to the solvation of ligand-protein complexes. J Chem Inf Model 2011;51:1867–1881.
31. Matsuoka D, Nakasako M. Prediction of hydration structures around hydrophilic surfaces of proteins by using the empirical hydration distribution functions from a database analysis. J Phys Chem B 2010;114:4652–4663.
32. Schymkowitz JW, Rousseau F, Martins IC, Ferkinghoff-Borg J, Stricher F, Serrano L. Prediction of water and metal binding sites and their affinities by using the Fold-X force field. Proc Natl Acad Sci U S A 2005;102:10147–10152.
33. Zheng M, Li Y, Xiong B, Jiang H, Shen J. Water PMF for predicting the properties of water molecules in protein binding site. J Comput Chem 2013;34:583–592.
34. Kramer C, Gedeck P. Three descriptor model sets a high standard for the CSAR-NRC HiQ benchmark. J Chem Inf Model 2011;51: 2139–2145.
35. Van Der Spoel D, Lindahl E, Hess B, Groenhof G, Mark AE, Berendsen HJ. GROMACS: fast, flexible, and free. J Comput Chem 2005;26:1701–1718.
36. Hornak V, Okur A, Rizzo RC, Simmerling C. HIV-1 protease flaps spontaneously close to the correct structure in simulations following manual placement of an inhibitor into the open state. J Am Chem Soc 2006;128:2812–2813.
37. Jorgensen WL, Chandrasekhar J, Madura JD, Impey RW, Klein ML. Comparison of simple potential functions for simulating liquid water. J Chem Phys 1983;79:926–935.
38. Wang J, Wolf RM, Caldwell JW, Kollman PA, Case DA. Development and testing of a general amber force field. J Comput Chem 2004;25:1157–1174.
39. Sciortino F, Essmann U, Stanley HE, Hemmati M, Shao J, Wolf GH, Angell CA. Crystal stability limits at positive and negative pressures, and crystal-to-glass transitions. Phys Rev E Stat Phys Plasmas Fluids Relat Interdiscip Topics 1995;52:6484–6491.
40. Hess B, Bekker H, Berendsen HJC, Fraaije JGEM. LINCS: A linear constraint solver for molecular simulations. J Comput Chem 1997; 18:1463–1472.
41. Ben-Naim A, Marcus Y. Solvation thermodynamics of nonionic solutes. J Chem Phys 1984;81:2016–2027.
42. Lorber DM, Shoichet BK. Flexible ligand docking using conformational ensembles. Protein Sci 1998;7:938–950.
43. Wei BQ, Weaver LH, Ferrari AM, Matthews BW, Shoichet BK. Testing a flexible-receptor docking algorithm in a model binding site. J Mol Biol 2004;337:1161–1182.
44. Mysinger MM, Shoichet BK. Rapid context-dependent ligand desolvation in molecular docking. J Chem Inf Model 2010;50:1561–1573.
45. Huggins DJ, Payne MC. Assessing the accuracy of inhomogeneous fluid solvation theory in predicting hydration free energies of simple solutes. J Phys Chem B 2013;117:8232–8244.
46. Huang N, Shoichet BK, Irwin JJ. Benchmarking sets for molecular docking. J Med Chem 2006;49:6789–6801.
47. Mysinger MM, Carchia M, Irwin JJ, Shoichet BK. Directory of useful decoys, enhanced (DUD-E): better ligands and decoys for better benchmarking. J Med Chem 2012;55:6582–6594.
48. Irwin JJ, Shoichet BK, Mysinger MM, Huang N, Colizzi F, Wassam P, Cao Y. Automated docking screens: a feasibility study. J Med Chem 2009;52:5712–5720.
49. Jacobson MP, Pincus DL, Rapp CS, Day TJ, Honig B, Shaw DE, Friesner RA. A hierarchical approach to all-atom protein loop prediction. Proteins 2004;55:351–367.
50. Li X, Jacobson MP, Friesner RA. High-resolution prediction of protein helix positions and orientations. Proteins 2004;55:368–382.
51. Huang N, Kalyanaraman C, Bernacki K, Jacobson MP. Molecular mechanics methods for predicting protein-ligand binding. Phys Chem Chem Phys 2006;8:5166–5177.
52. Pettersen EF, Goddard TD, Huang CC, Couch GS, Greenblatt DM, Meng EC, Ferrin TE. UCSF Chimera-a visualization system for exploratory research and analysis. J Comput Chem 2004;25:1605–1612.
53. Carugo O, Bordo D. How many water molecules can be detected by protein crystallography? Acta Crystallogr D Biol Crystallogr 1999; 55(Pt 2):479–483.
54. Yan A, Grant GH, Richards WG. Dynamics of conserved waters in human Hsp90: implications for drug design. J R Soc Interface 2008; 5 Suppl 3:S199–205.
55. Merkel AL, Meggers E, Ocker M. PIM1 kinase as a target for cancer therapy. Expert Opin Investig Drugs 2012;21:425–436.
56. Cao R, Liu M, Yin M, Liu Q, Wang Y, Huang N. Discovery of novel tubulin inhibitors via structure-based hierarchical virtual screening. J Chem Inf Model 2012;52:2730–2740.
57. Saxena AK, Roy KK. Hierarchical virtual screening: identification of potential high-affinity and selective beta(3)-adrenergic receptor agonists. SAR QSAR Environ Res 2012;23:389–407.
58. Liu X, Xie H, Luo C, Tong L, Wang Y, Peng T, Ding J, Jiang H, Li H. Discovery and SAR of thiazolidine-2,4-dione analogues as insulin-like growth factor-1 receptor (IGF-1R) inhibitors via hierarchical virtual screening. J Med Chem 2010;53:2661–2665.
59. Christofferson A, Zhao L, Sun H, Huang Z, Huang N. Theoretical studies of the base pair fidelity of selenium-modified DNA. J Phys Chem B 2011;115:10041–10048.